UNIVERSITY OF VICTORIA

CENTRE FOR EARTH AND OCEAN RESEARCH (CEOR)

Mixing in the Upper Ocean

by:

H. Yamazaki

CEOR Report: 96-1

April 1996

Postal Address:

University of Victoria
P.O. Box 3055
Victoria, British Columbia
Canada V8W 3P6

Tel: (604) 721-8848
Fax: (604) 472-4100

DISCLAIMER NOTICE

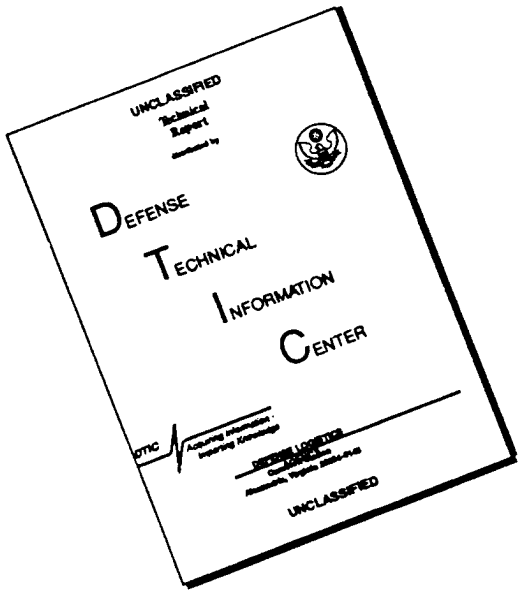

THIS DOCUMENT IS BEST QUALITY AVAILABLE. THE COPY FURNISHED TO DTIC CONTAINED A SIGNIFICANT NUMBER OF PAGES WHICH DO NOT REPRODUCE LEGIBLY.

Mixing in the Upper Ocean

by:

H. Yamazaki

CEOR Report: 96-4

April 1996

An Observation of Gravitational Collapse Caused by Turbulent Mixing

Hidekatsu Yamazaki
Department of Marine Science and Technology
Tokyo University of Fisheries
4-5-7 Konan, Minato-ku Tokyo 108, Japan

and

Centre for Earth and Ocean Research
University of Victoria
P.O. Box 1700
Victoria, B.C. V8W 2Y2, Canada

September 14 1994, submitted
May 22, 1995, revised
October 9, 1995, final revision

Journal of Physical Oceanography

Abstract

A turbulent mixing layer, presumed to be caused by strong shear due to inertial waves, was observed from the research submarine *USS Dolphin*. As a consequence of the mixing, a density flux was set up. Although inertial waves exhibit motion on a much larger scale than turbulence, the horizontal extent of the waves has a limit. Therefore, a gravitational imbalance between the turbulent layer and its outside is expected. Data indicated that the gravitational imbalance created an intrusion, at the head of which high wavenumber internal waves were observed.

1. Introduction

Atmospheric disturbances, such as the passage of a storm, in the open ocean often cause inertial waves to propagate downward (Price 1983; Pollard 1970; Pollard and Millard 1970; D'Asaro 1985, 1989). Since the physical scales of inertial waves are at least several kilometers and the total amount of energy is very high, the associated shear can induce a persistent turbulent layer (Itsweire et al. 1989; Hebert and Moum 1994). Usually the vertical group speed of near-inertial waves is an order of several meters per day, thus the associated disturbance propagates slowly in the water column. Although inertial waves have been observed at all levels of the open ocean water column (Sanford 1991), turbulence caused by near-inertial waves rapidly dissipates the kinetic energy of the wave (Eriksen 1991; Hebert and Moum 1994).

Regarding turbulent mixing events induced by near-inertial waves, we need to bear two facts in mind: (1) the inertial wave has a limited horizontal scale and (2) turbulence elevates the potential energy of the water column. Hence we can expect that the horizontally limited water column with higher potential energy than the surrounding water column may cause a gravitational collapse. In fact, multisensor observations in the atmosphere (Mahapatra et al. 1991) clearly showed an undular bore generated from a storm mixing event, and upstream disturbances were observed in front of the bore. A similar phenomenon known as "the morning glory" has also been reported (e.g. Smith et al. 1982). If the same scenario is applied to the ocean, turbulent mixing is not the end of the energy cascade. The vertical density flux due to turbulent mixing may be a source of energy for a gravitational collapse and soliton-like waves can be generated from the upstream disturbance, as has been observed in a laboratory (Maxworthy 1980; Amen and Maxworthy 1980). This process can generate high wavenumber internal waves away from the solid boundary in the central area of the open ocean.

The events of a scenario are illustrated in Figure 1. The whole process is as follows:

1. an atmospheric disturbance causes an inertial wave;

2. turbulence is driven by the inertial wave shear;

3. vertical density fluxes result from the mixing;

4. a gravitational imbalance in the horizontal direction induces an intrusion;

5. high wavenumber internal waves are generated at the head of the intrusion.

Making use of data published by Yamazaki and Osborn (1993), evidence has been found to justify the process described above. The next section briefly summarizes the data, with consistency tests presented in the following section.

2. Observed Data

Microstructure data were observed from the research submarine *USS Dolphin* which has a length of 51 m and a diameter of 5.6 m. Turbulence was measured at the top of a 4.7-m tripod placed near the bow of the submarine. Two airfoil probes were used to measure the vertical component, w, and the horizontal component, v, of turbulent velocity. Two high-response thermistors measured the temperature field adjacent to the airfoil probes. The hydrography was monitored from a CTD package mounted at the top of the tripod. Along the front leg of the tripod, six thermistors were mounted to resolve the vertical structure of stratification. A 1.2-MHz ADCP, with a 1-m resolution, was mounted in front of the tripod to monitor the shear field. Details of the instrumentation can be found in Yamazaki and Osborn (1993).

The data used in this paper come from part of a 7-h dive which took place off the coast of San Diego, California. The distance to the shore was about 30 Km, and the depth generally exceeded 800m. Two ascending and two descending legs of the tripod located between the surface and about 50 m in depth provided the vertical structure of the background stratification. Although the dive took place at night, the effects from convective cooling was limited to above 30 m (Figure 2). During 0950 and 1030 UTC, we encountered a vigorous shear layer with the shear sufficiently strong enough to induce an energetic mixing event (Yamazaki and Osborn 1993). The turbulent shear layer had a thickness of about 5 m and was located in a seasonal thermocline (Figure 2). Because the salinity contribution to the density was minimal, as discussed in Yamazaki and

Osborn (1993), the thermal structure obtained from a thermistor chain provided a picture of the local stratification.

A 2400-s data segment was extracted from the whole dive. Since the nominal speed of the *Dolphin* was 1.5 m s^{-1}, the displayed segment corresponds to 3600 m. The thermal structure was monitored from the thermistor chain (Figure 3a). Turbulence was measured along the solid line at the top of the temperature contour. Figure 3b shows the high shear region identified from ADCP data. Again, the solid line in this figure shows the location where turbulence was observed. Both the rate of dissipation of kinetic energy, ϵ, and the temperature gradient dissipation rate, χ, were used to infer the mixing layer shown in this figure. The local hydrography conditions, i.e. the local gradient Richardson number, Ri, the square of the horizontal shear, S_H, the local buoyancy frequency, N, salinity, S, density, σ_t, and temperature, T, were computed from the CTD data set and 10-s average ADCP data. See details of the data processing in Yamazaki and Osborn (1993).

3. Consistency Tests

In order to identify the source of the horizontal shear, two sections of the shear vector field were examined: 1) between the elapsed time of 500 and 1000 s, where the turbulence probes were in the mixing layer and 2) between the elapsed time of 1200 and 1500 s, where the shear magnitude contour is the most contiguous. The shear vector measured from the direction of the submarine operation showed -120 at the top of the layer to -80 toward the bottom layer for both sections (Figure 4). This shear field is consistent with a downward-propagating inertial wave. From a previous experiment in the same area (Yamazaki and Lueck 1987) a persistent shear layer was found at roughly 200 m at an interface between the California current and the California undercurrent. No shear layer due to any other type of flow system is recognized above 100 m. Therefore, the observed shear layer is due to a near-inertial wave generated from an atmospheric disturbance. Similar features are reported in Itsweire et al. (1989) and Hebert and Moum (1994). If this inertial wave was topographically generated from a tidal forcing,

the wave would have traveled through the entire water column, and then reflected back from the surface. Such a wave would have exhausted the mechanical energy substantially. Thus, considering the intensity of turbulence associated with the shear, the observed intertial wave is not originated from a topography.

Did the shear last long enough to create a "mixed" layer appearing in the data? In order to test this notion, the mixing time scale of the turbulent layer was estimated using the following simple temperature equation

$$\frac{\partial T_0}{\partial t} = -\frac{\partial \langle u_j' T' \rangle}{\partial x_j} - u_H \frac{\partial T_0}{\partial x_H} \tag{1}$$

where T_0 is the mean background temperature, u_H is the horizontal component of the mean velocity, u_j' are turbulent velocity components with the standard index notation, and T' is the fluctuating temperature component.

If the mixing field is horizontally homogenous and no interfacial entrainment is taking place, the vertical heat flux term on the right hand side of equation (1) dominates the rest of the terms. Then the balance equation becomes

$$\begin{aligned} \frac{\partial T_0}{\partial t} &= -\frac{\partial \langle u_3' T' \rangle}{\partial x_3} \\ &= -\frac{\partial \langle w T' \rangle}{\partial z} \end{aligned} \tag{2}$$

so that the mixing time scale, t_{mix}, may be estimated from the following discrete form

$$\frac{\Delta T}{t_{\mathrm{mix}}} = \frac{\langle w T' \rangle}{\Delta z} \tag{3}$$

where ΔT is the temperature difference between the top and the bottom of the mixing layer, and Δz is half of the mixing layer thickness. The observed values shown in Table 1 give $t_{\mathrm{mix}} = 106$ h. Since this time scale is solely based on the observed vertical heat flux, this time scale may be considered to be the upper bound for the mixing time scale.

Because the edge of the mixing layer was observed, we cannot assume the horizontal homogeneity of the mixing layer. Therefore, the advection terms as well as the horizontal flux terms should be taken into consideration. In order to account for these terms, the heat flux through

the density interface at the bottom of the mixed layer is estimated. The reason for doing so is that both the horizontal terms and the vertical fluxes within the mixed layer should result from the heat flux through the interface. An attempt to calculate the heat flux is made using the eddy diffusivity method of Osborn and Cox (1972). Since the vertical flux within the mixing layer has been observed (Yamazaki and Osborn 1993), the eddy diffusivity can be estimated from

$$K_T = -\frac{\langle wT' \rangle}{(\partial T_0/\partial z)_m} \tag{4}$$

where $(\partial T_0/\partial z)_m$ is the temperature gradient in the mixing layer, and the heat flux through the interface is expressed as

$$-\langle wT' \rangle = K_T \left(\frac{\partial T_0}{\partial z}\right)_i \tag{5}$$

where $(\partial T_0/\partial z)_i$ is the temperature gradient at the bottom of the mixing layer interface. Here the eddy diffusivity at the interface is assumed to be identical to the eddy diffusivity in the mixing layer. The mean background temperature gradient in the mixed layer is $0.03°\mathrm{C\ m^{-1}}$, so K_T is $8 \times 10^{-5}\ \mathrm{m^2\ s^{-1}}$. Making use of this coefficient, the heat flux at the density interface is expected to be $4.4 \times 10^{-5}\ \mathrm{°C\ m\ s^{-1}}$, so the mixing time scale becomes 3.9 h. At least this is the minimum time scale to create the mixed layer. In order to induce gravitational collapse, turbulent mixing must persist longer than this time scale. Thus, this is the lower bound for the mixing time scale. Since inertial wave energy, in general, propagates at several meters per day, the true mixing time scale is in a reasonable range specified by the upper and the lower bound time scale.

Although the submarine fluctuated slightly between 37 and 41 m, both inside (0–1000 s) and outside (1600–2400 s) of the mixing layer were observed at roughly the same depth. The difference in σ_t between the inside and outside of the mixing layer is about 0.05, so the water column is gravitationally unstable in the horizontal direction. Therefore, it is not unreasonable to expect a gravitational collapse caused by the turbulent mixing layer. The gravitational collapse causes an intrusion into a stratified fluid. The intrusion takes place from left to right in Figure

3, so internal waves between the elapsed time of 1200 and 1500 s are associated with the head of the intrusion.

In general, the intrusion speed cannot exceed a critical speed of gravity current C_G

$$C_G = \left(\frac{\Delta\rho}{\rho_0 g h}\right)^{1/2} \tag{6}$$

where h is the thickness of the gravity current, $\Delta\rho$ is the difference between the gravity current and the ambient water, ρ_0 is the ambient water density, and g is the gravitational acceleration. So the intrusion speed C_I should be less than $C_G = 0.05$ m s^{-1}.

$$C_I < C_G. \tag{7}$$

The observed internal waves and the intrusion are consistent with the laboratory experiment of Amen and Maxworthy (1980) who found a series of solitary waves generated from the head of a gravitationally collapsed mixed layer. The largest amplitude internal wave had an apparent wave length of roughly $L_a = 70$ m. Since we cannot infer at what angle the submarine crossed the internal waves, the actual wave length should be less than the apparent one. Making use of the observed stratification at this point of the water column, $N = 0.01$ s^{-1}, the maximum phase speed of this wave is

$$C_{\max} = L_a N/2\pi = 0.11 \text{ m s}^{-1}. \tag{8}$$

The largest observed wave height is roughly 3 m, so the minimum wave length, $L_{\min}$, corresponding to the steepest wave slope, $0.34/\pi$, (Thorpe 1978) is roughly 30 m. Hence the minimum phase speed, $C_{\min}$, is 0.05 m s^{-1}. The actual phase speed, C, should be between $C_{\min}$ and $C_{\max}$:

$$C_{\min} < C < C_{\max}. \tag{9}$$

Therefore, observed internal waves are propagating faster than the intrusion.

Based on the foregoing consistency test, it is concluded that the proposed energy cascade is a plausible process in the ocean. The implication of this result is that turbulence mixing can cause a secondary process, i.e. the intrusion due to gravitational collapse.

Acknowledgments. I thank S. Garrett for drawing Figure 1. My appreciation is also extended to two conscientious anonymous reviewers, who provided valuable comments, and to R. Rutka, who edited this manuscript. This work was supported by grants from the Office of Naval Research.

References

Amen, R., and T. Maxworthy, 1980: The gravitational collapse of a mixed region into a linearly stratified fluid. *J. Fluid Mech.*, **96,** 65–80.

D'Asaro, E. A., 1985: The energy flux from the wind to near-inertial motions in the surface mixed layer. *J. Phys. Oceanogr.*, **15,** 1043–1059.

D'Asaro, E. A., 1989: The decay of wind-forced mixed layer inertial oscillations due to the β effect. *J. Geophys. Res.*, **94,** 2045–2056.

Eriksen, C. C., 1991: Observations of near-inertial internal waves and mixing in the seasonal thermocline. *Dynamics of Oceanic Internal Gravity Waves,* Proceedings of 'Aha Huliko'a Hawaiian Winter Workshop, P. Müller and D. Henderson Eds., Hawaii Institute of Geophysics, Honolulu, 71–88.

Hebert, D., and J. N. Moum, 1994: Decay of a near-inertial wave. *J. Phys. Oceanogr.*, **24,** 2334–2351.

Itsweire, E. C., T. R. Osborn, and T. P. Stanton, 1989: Horizontal distribution and characteristics of shear layers in the seasonal thermocline. *J. Phys. Oceanogr.*, **19,** 301–320.

Mahapatra, P. R., R. J. Doviak, and D. S. Zrnic, 1991: Multisensor observation of an atmospheric undular bore. *Bull. Amer. Met. Soc.*, **72,** 1468–1480.

Maxworthy, T., 1980: On the formation of nonlinear internal solitary waves from the gravitational collapse of mixed regions in two and three dimensions. *J. Fluid Mech.*, **96,** 47-64.

Osborn, T. R. and C. S. Cox, 1972: Oceanic fine structure. *Geophys. Fluid Dyn.*, **3,** 321–345.

Pollard, R. T., 1970: On the generation by winds of inertial waves in the ocean. *Deep-Sea Res.*, **17,** 795–812.

Pollard, R. T., and R. C. Millard 1970: Comparison between observed and simulated wind-generated interial oscillations. *Deep-Sea Res.*, **17,** 813–821.

Price, J. F., 1983: Internal wave wake of a moving storm. Part 1: Scales, energy budget and observations. *J. Phys. Oceanogr.*, **13,** 949–965.

Sanford, T.B., 1991: Spatial structure of thermocline and abyssal internal waves. *Dynamics of Oceanic Internal Gravity Waves,* Proceedings of 'Aha Huliko'a Hawaiian Winter Workshop, P. Müller and D. Henderson Eds., Hawaii Institute of Geophysics, Honolulu, 109–141.

Smith, R. K., N. Crook, and G. Roff, 1982: The Morning Glory: An extraordinary atmospheric undular bore. *Quart. J. R. Met. Soc.,* **108,** 937–956.

Thorpe, S. A. 1978: On the shape and breaking of finite amplitude internal gravity waves in a shear flow. *J. Fluid Mech.,* **85,** 7–31.

Yamazaki, H., and R. G. Lueck, 1987: Turbulence in the California undercurrent. *J. Phys. Oceanogr.,* **17**, 1378–1396.

Yamazaki, H., and T. R. Osborn, 1993: Direct estimation of heat flux in a seasonal thermocline. *J. Phys. Oceanogr.,* **23**, 503–516.

Table 1. Observed values associated with the mixing layer.

Parameter	Value
$\langle w'T' \rangle$	1.63×10^{-6} °C m s^{-1}
ΔT	0.25 °C
$\Delta \rho$	0.05 kg m^{-3}
h	5 m
$(\partial T_0/\partial z)_m$	0.03 °C m^{-1}
$(\partial T_0/\partial z)_i$	0.55 °C m^{-1}

Figure 1. Illustration depicting the energy cascade proposed in this paper. An atmospheric disturbance generates near-inertial waves whose group speed $\mathbf{C_g}$ is almost vertical and whose frequency is roughly local f. Shear associated with the inertial wave causes turbulent mixing and induces the density flux $\langle w\rho \rangle$. The flux reaches a gravitational collapse of the mixed layer; as a result, the head of the intrusion causes the upstream disturbance generating high wavenumber internal waves.

Figure 2. Temperature profiles obtained from the second descending (thick curve) and the second ascending (thin curve) sections of the dive. A shear layer was observed between 35 and 45 m during the descending section, and no shear layer was observed during the ascending section.

Figure 3. Hydrographic conditions associated with the turbulent mixing layer. (a) Thermal structures identified with a thermistor chain. The temperature contour interval is 0.05°C. Making use of turbulent dissipation rate data, the depicted mixing area is shown with hatches. (b) Shear contours. Two levels of shear contour are shown: $S_H^2 = 4 \times 10^{-4}$ s^{-2} and 8×10^{-4} s^{-2}. The shaded area depicts the high shear region. Thick solid line in (a) and (b) is the location of the turbulence package. (c) The dissipation rate of thermal variance χ. (d) The rate of dissipation of kinetic energy, ϵ. (e) Local gradient Richardson number, Ri. (f) Local shear squared value, S_H^2. (g) Salinity, S. (h) σ_t. (i) Temperature, T. (j) Local buoyancy frequency, N^2.

Figure 4. Contours of the direction of the shear vector are drawn for (a) elapsed time between 500 and 1000, and (b) between 1200 and 1700. The angle is measured in the horizontal plane, relative to the direction of submarine travel, x, as shown in (c). The shear vector rotates clockwise as it descends. The background contours in (a) and (b) show the magnitude of shear squared appearing in Figure 3b. The location of the turbulence package is shown with dashed line.

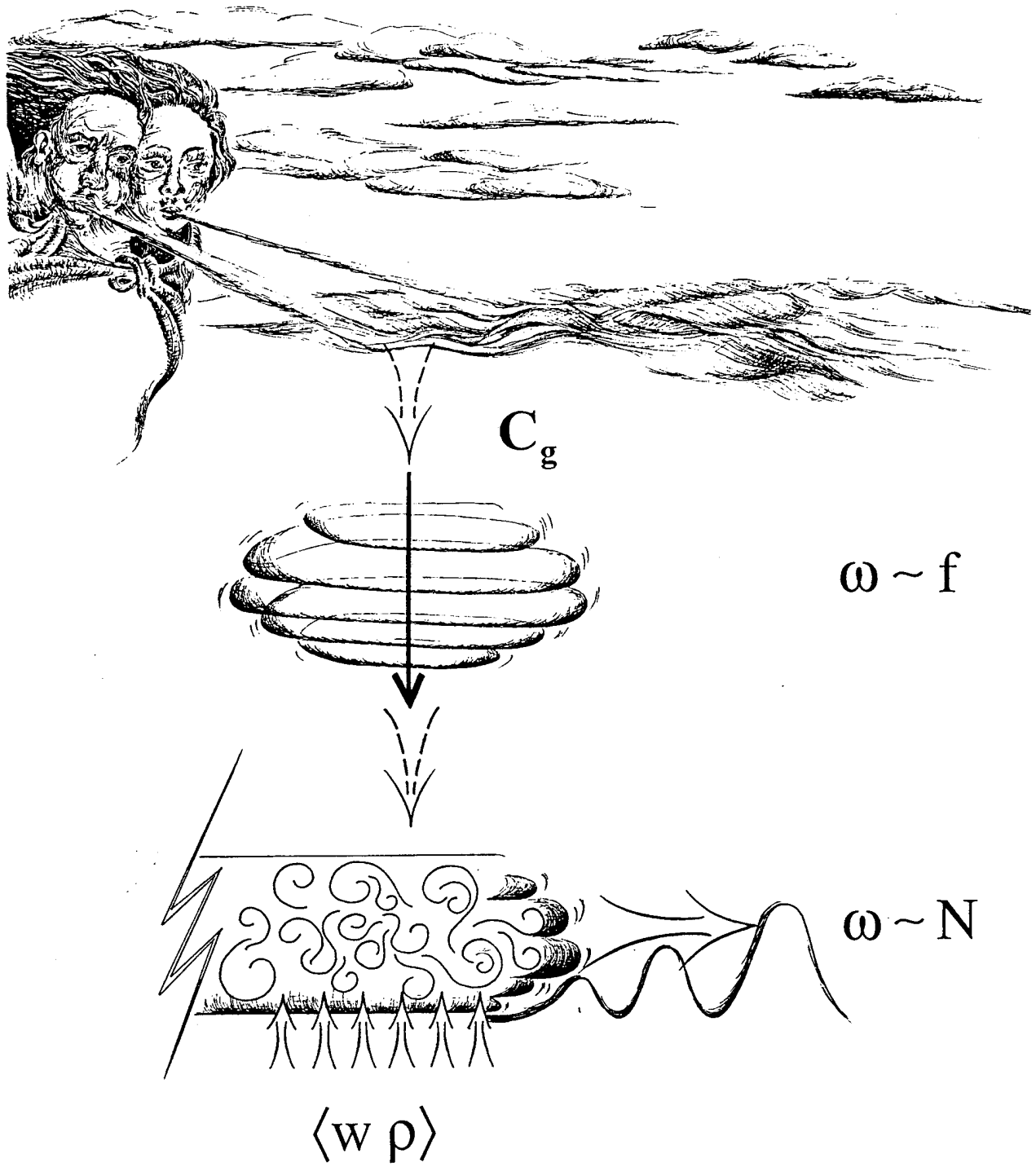
C_g
$\omega \sim f$
$\omega \sim N$
$\langle w \rho \rangle$

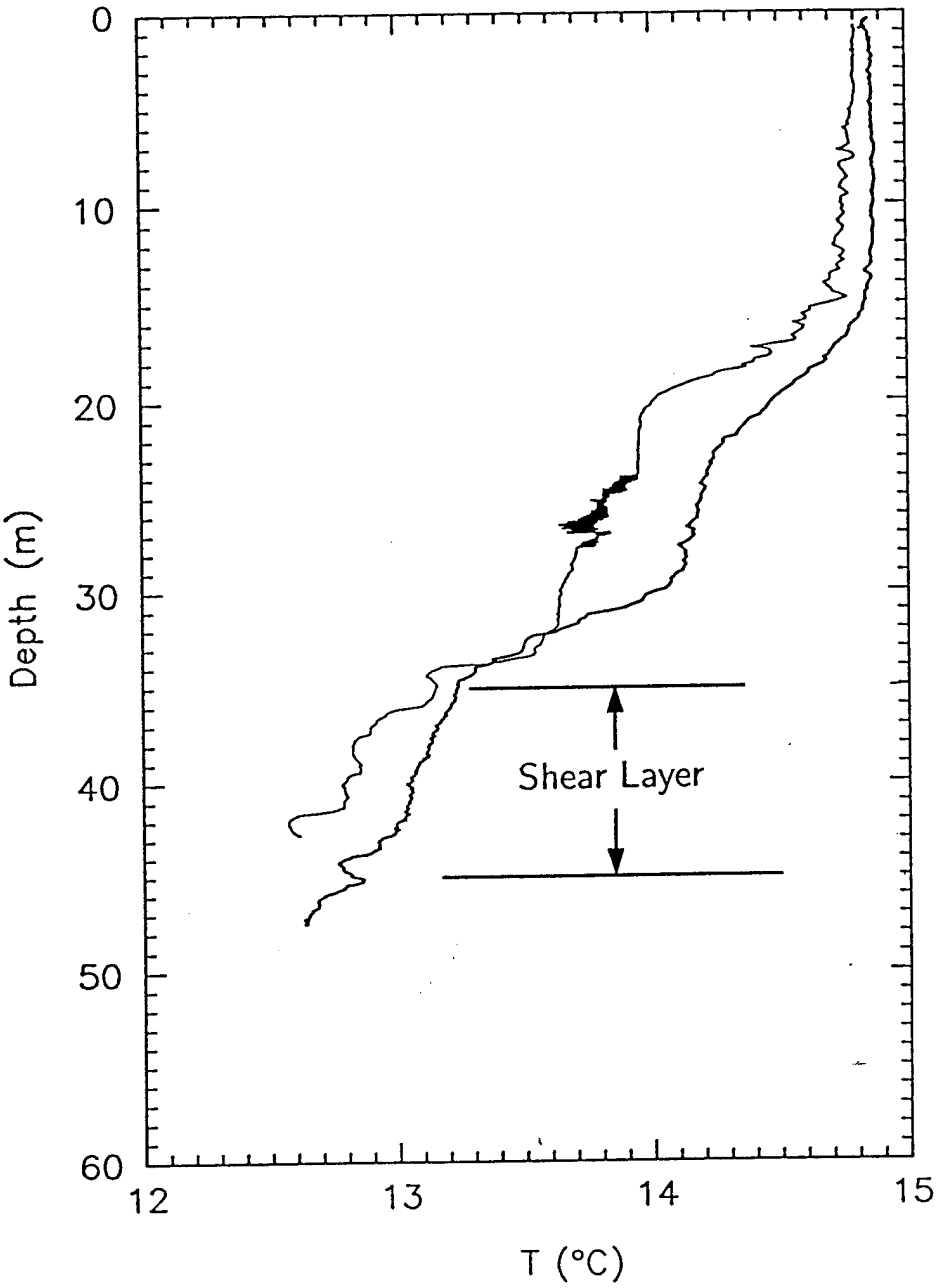

Figure 7.

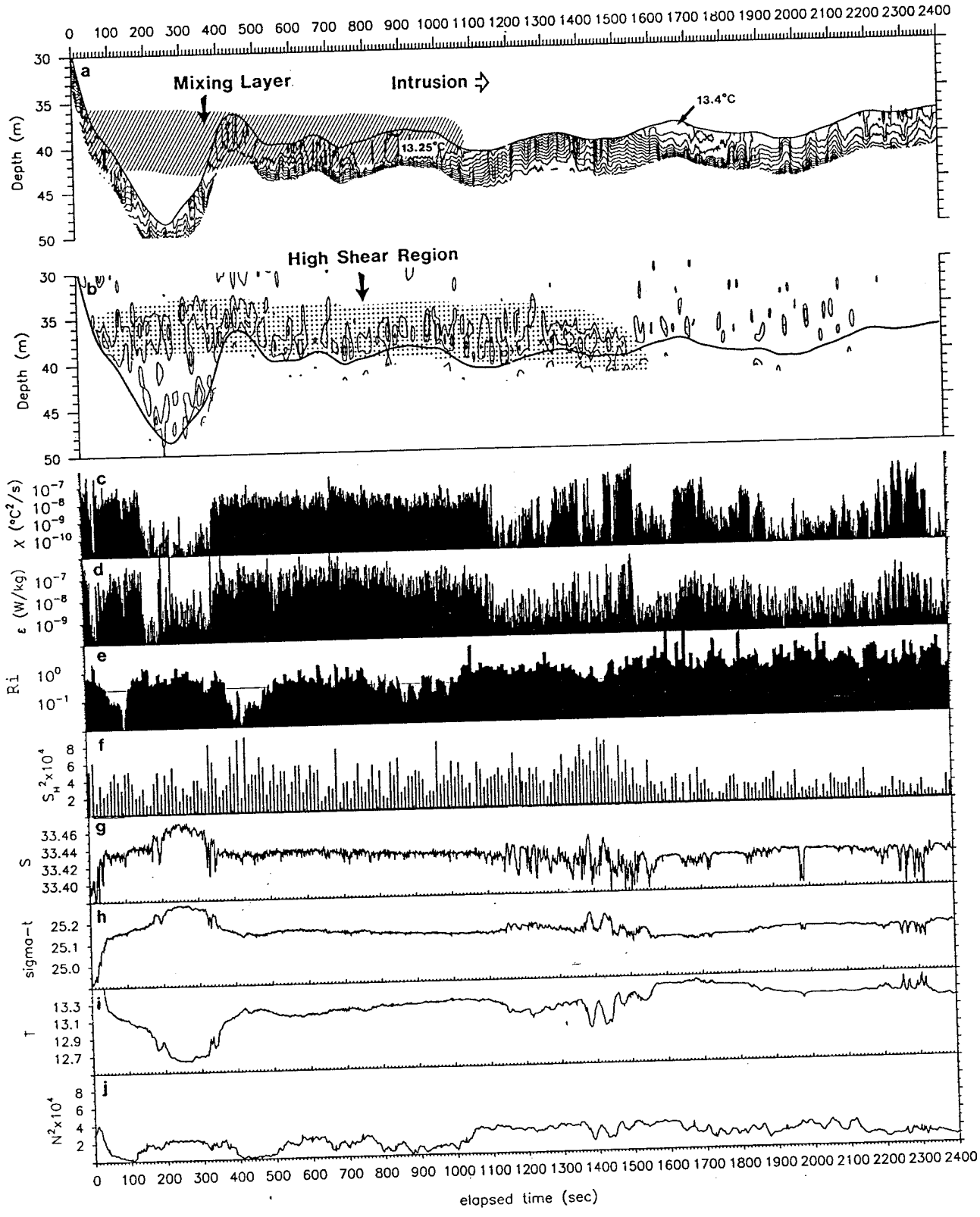
Mixing Layer
Intrusion
13.4°C
13.25°C
High Shear Region
Depth (m)
χ (°C²/s)
ε (W/kg)
Ri
S
sigma-t
T
N²x10⁴
elapsed time (sec)

Figure 3

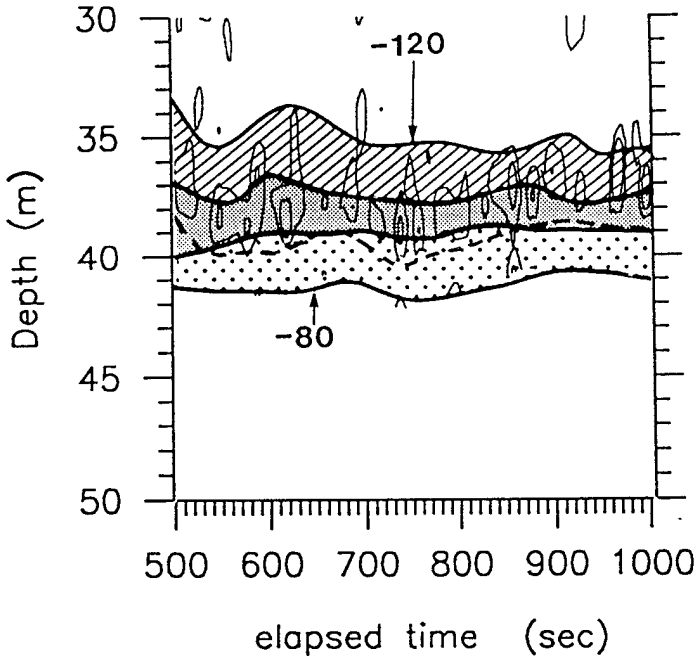
30
35
40
45
50
Depth (m)
-120
-80
500 600 700 800 900 1000
elapsed time (sec)

Figure 4.a

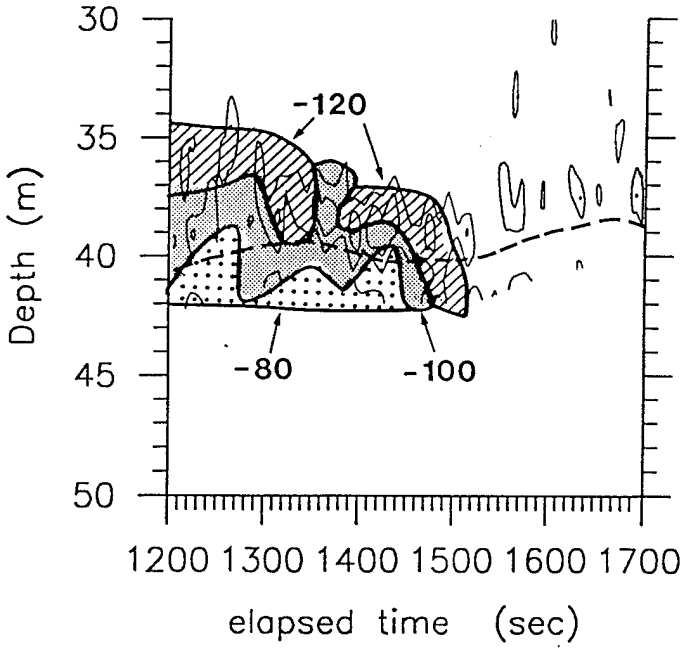
30
35
40
45
50
Depth (m)
-120
-80
-100
1200 1300 1400 1500 1600 1700
elapsed time (sec)

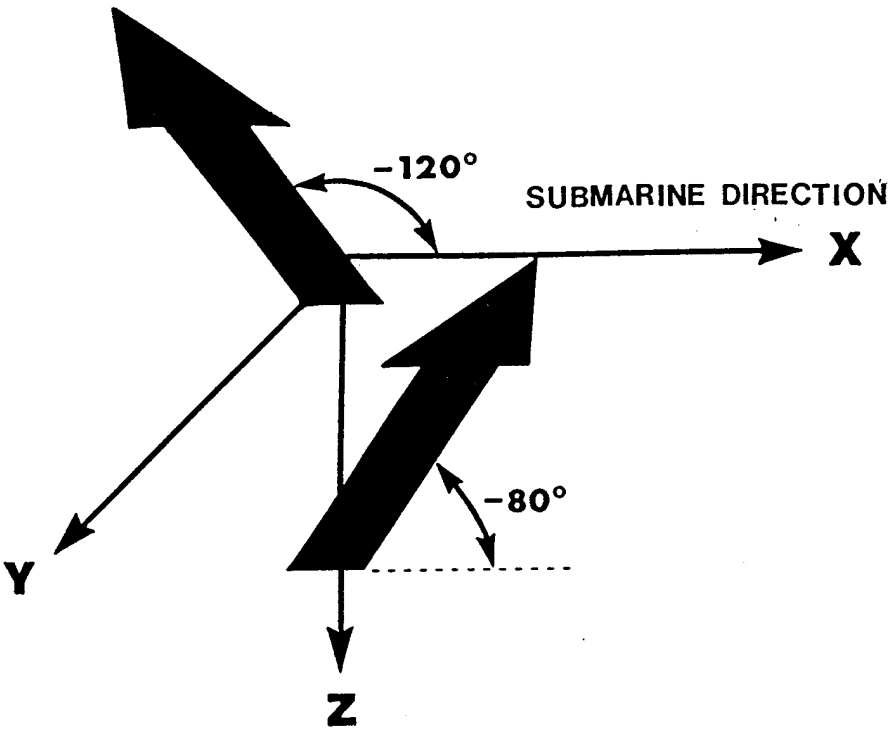

Figure 4.c

REPORT DOCUMENTATION PAGE

Form Approved
OMB No. 0704-0188

1. AGENCY USE ONLY (Leave blank)	2. REPORT DATE	3. REPORT TYPE AND DATES COVERED
	30 March 1996	Final: 01 Feb 1993 - 31 Jan 1995

4. TITLE AND SUBTITLE

Mixing in the upper ocean

5. FUNDING NUMBERS

G-N00014-93-1-0357

6. AUTHOR(S)

Hidekatsu Yamazaki

7. PERFORMING ORGANIZATION NAME(S) AND ADDRESS(ES)

Centre for Earth and Ocean Research
University of Victoria
P.O. Box 1700
Victoria, B.C., V8W 2Y2, Canada

8. PERFORMING ORGANIZATION REPORT NUMBER

9. SPONSORING/MONITORING AGENCY NAME(S) AND ADDRESS(ES)

Department of the Navy
Office of Chief of Naval Research
800 Quincy Street, Code 1512 AW
Arlington, Virginia, 22217-5000

10. SPONSORING/MONITORING AGENCY REPORT NUMBER

11. SUPPLEMENTARY NOTES

will appear in Journal of Physical Oceanography

12a. DISTRIBUTION/AVAILABILITY STATEMENT

Unlimitted Availability

12b. DISTRIBUTION CODE

13. ABSTRACT *(Maximum 200 words)*

A turbulent mixing layer, presumed to be caused by strong shear due to inertial waves, was observed from the research submarine USS Dolphin. As a consequence of the mixing, a density flux was set up. Although inertial waves exhibit motion on a much larger scale than turbulence, the horizontal extent of the waves has a limit. Therefore, a gravitational imbalance between the turbulent layer and the outside is expected. Data indicated that the gravitational imbalance created an intrusion, at the head of which high wavenumber internal waves were observed.

14. SUBJECT TERMS

Turbulence, internal waves, mixing

15. NUMBER OF PAGES

20

16. PRICE CODE

17. SECURITY CLASSIFICATION OF REPORT	18. SECURITY CLASSIFICATION OF THIS PAGE	19. SECURITY CLASSIFICATION OF ABSTRACT	20. LIMITATION OF ABSTRACT
UNCLASSIFIED	UNCLASSIFIED	UNCLASSIFIED	

GENERAL INSTRUCTIONS FOR COMPLETING SF 298

The Report Documentation Page (RDP) is used in announcing and cataloging reports. It is important that this information be consistent with the rest of the report, particularly the cover and title page. Instructions for filling in each block of the form follow. It is important to ***stay within the lines*** to meet ***optical scanning requirements***.

Block 1. Agency Use Only *(Leave blank)*.

Block 2. Report Date. Full publication date including day, month, and year, if available (e.g. 1 Jan 88). Must cite at least the year.

Block 3. Type of Report and Dates Covered. State whether report is interim, final, etc. If applicable, enter inclusive report dates (e.g. 10 Jun 87 - 30 Jun 88).

Block 4. Title and Subtitle. A title is taken from the part of the report that provides the most meaningful and complete information. When a report is prepared in more than one volume, repeat the primary title, add volume number, and include subtitle for the specific volume. On classified documents enter the title classification in parentheses.

Block 5. Funding Numbers. To include contract and grant numbers; may include program element number(s), project number(s), task number(s), and work unit number(s). Use the following labels:

C	- Contract	**PR**	- Project
G	- Grant	**TA**	- Task
PE	- Program Element	**WU**	- Work Unit Accession No.

Block 6. Author(s). Name(s) of person(s) responsible for writing the report, performing the research, or credited with the content of the report. If editor or compiler, this should follow the name(s).

Block 7. Performing Organization Name(s) and Address(es). Self-explanatory.

Block 8. Performing Organization Report Number. Enter the unique alphanumeric report number(s) assigned by the organization performing the report.

Block 9. Sponsoring/Monitoring Agency Name(s) and Address(es). Self-explanatory.

Block 10. Sponsoring/Monitoring Agency Report Number. (If known)

Block 11. Supplementary Notes. Enter information not included elsewhere such as: Prepared in cooperation with ...; Trans. of ...; To be published in .... When a report is revised, include a statement whether the new report supersedes or supplements the older report.

Block 12a. Distribution/Availability Statement. Denotes public availability or limitations. Cite any availability to the public. Enter additional limitations or special markings in all capitals (e.g. NOFORN, REL, ITAR).

- **DOD** - See DoDD 5230.24, "Distribution Statements on Technical Documents."
- **DOE** - See authorities.
- **NASA** - See Handbook NHB 2200.2.
- **NTIS** - Leave blank.

Block 12b. Distribution Code.

- **DOD** - Leave blank.
- **DOE** - Enter DOE distribution categories from the Standard Distribution for Unclassified Scientific and Technical Reports.
- **NASA** - Leave blank.
- **NTIS** - Leave blank.

Block 13. Abstract. Include a brief *(Maximum 200 words)* factual summary of the most significant information contained in the report.

Block 14. Subject Terms. Keywords or phrases identifying major subjects in the report.

Block 15. Number of Pages. Enter the total number of pages.

Block 16. Price Code. Enter appropriate price code *(NTIS only)*.

Blocks 17. - 19. Security Classifications. Self-explanatory. Enter U.S. Security Classification in accordance with U.S. Security Regulations (i.e., UNCLASSIFIED). If form contains classified information, stamp classification on the top and bottom of the page.

Block 20. Limitation of Abstract. This block must be completed to assign a limitation to the abstract. Enter either UL (unlimited) or SAR (same as report). An entry in this block is necessary if the abstract is to be limited. If blank, the abstract is assumed to be unlimited.